Cite as: J. E. Cole *et al.*, *Science*
10.1126/science.ady2660 (2026).

Recent strengthening of eastern Pacific ENSO in the last millennium paleorecord

J. E. Cole[1]*, D. M. Thompson[2], K. A. Dyez[1], C. J. Tripp[1], A. W. Tudhope[3], M. Lofverstrom[2], S. Stevenson[4], J. M. Okun[1], A. E. Lawman[5], J. L. Conroy[6], J. T. Overpeck[7], G. Jimenez[8], R. L. Edwards[9]

[1]Department of Earth and Environmental Sciences, University of Michigan, Ann Arbor, MI, USA. [2]Department of Geosciences, University of Arizona, Tucson, AZ, USA. [3]School of GeoSciences, University of Edinburgh, Scotland, UK. [4]Bren School of Environmental Sciences and Management, University of California, Santa Barbara, CA, USA. [5]Environmental Studies and Science Program, Colorado College, Colorado Springs, CO, USA. [6]Department of Earth Science and Environmental Change, University of Illinois at Urbana-Champaign, Urbana, IL, USA. [7]School of Environment and Sustainability, University of Michigan, Ann Arbor, MI, USA. [8]Moody's Risk Management Services. [9]Department of Earth and Environmental Sciences, University of Minnesota, Minneapolis, MN, USA.

***Corresponding author. Email: colejul@umich.edu**

The Pacific El Niño–Southern Oscillation (ENSO) generates climate extremes that endanger ecosystems, infrastructure, and human well-being worldwide. The response of this system to climate warming is poorly constrained, due both to data scarcity and uncertainties in climate models. The geochemistry of Galápagos coral skeletons across the past millennium reveals a large recent increase in interannual variability of sea surface temperature in the eastern equatorial Pacific compared to existing paleorecords that exceeds simulated natural variability. This increase parallels rising global temperature and results from stronger El Niño events. Central Pacific coral data also show increased variability, although less distinctly than in the Galápagos. Our results provide long-term context for understanding ENSO variability trends, with troubling implications for climate extremes.

El Niño–Southern Oscillation (ENSO) is the leading source of interannual extremes in modern climate, linked to droughts, floods, infrastructural damages, coral bleaching, wildfires, and agricultural and health impacts (*1*–*3*). ENSO is defined by coupled variability of the ocean and atmosphere in the equatorial Pacific, emerging from multiple processes as a coherent pattern of changes in tropical Pacific sea surface temperature (SST) and associated wind, hydrologic, and oceanographic features (*4*, *5*). The complexity of the system, and remote influences, (*6*), create large internal variability that masks a clear response to external climate forcing (*7*–*9*) and hinders model projections, making the attribution of ENSO behavior to specific drivers and the projection of future extremes [CJ1.1]difficult. Thus there is a pressing need for more long-term observations from the equatorial Pacific to help constrain models, establish a better record of past ENSO variability, and provide context for its recent behavior. Here we report paleoclimate records from Galápagos corals (Fig. 1) that allow us to compare recent ENSO variability to that of the previous millennium.

Spatial and temporal ENSO variability

Several large and impactful El Niño events have occurred in recent decades, each exhibiting warming that extends from South America to the international dateline. This increase in strong, basin-wide El Niño events results in increasing skewness of eastern Pacific SST anomalies (*10*, *11*) (fig. S1). However, the large internal variability of ENSO and the sparse instrumental record (*12*) (fig. S1) complicate attribution of these trends to anthropogenic warming (*13*, *14*). The first systematic SST observations of the remote region defining ENSO variability (e.g., Niño 3.4: 5°S-5°N; 120-180°W) began in the 1980s with satellite observations, later augmented by the in-situ TOGA-TAO array (*1*).

Spatial variability complicates this picture: warm SST anomalies in the eastern Pacific (EP) are typically stronger than those in the central Pacific (CP) (*15*, *16*) or along the South American coastline (*17*). Spatial modes of ENSO may respond differently to changing climate forcing, e.g., over recent millennia (*18*, *19*), and under anthropogenic influences (*4*, *11*, *20*). Paleorecords from central Pacific corals are beginning to reveal long-term CP variability (*21*–*26*), but the EP lacks comparable data to place current trends in long-term context.

Model projections of future climate change tend to disagree on how ENSO-related SST variability will respond to climate warming. Using the latest coupled climate models (phases 5 and 6 of the Coupled Model Intercomparison Project, hereafter CMIP5/6), the 6th Assessment Report of the Intergovernmental Panel on Climate Change found no consensus on changing variability in central Pacific (Niño3.4) SST, even under high emissions scenarios (*7*). Later studies using a subset of models, and large single-model ensembles, identify increased ENSO SST variability under anthropogenic forcing (*27*, *28*). In studies that distinguish EP and CP modes, most CMIP5/6 models show a forced increase in ENSO-SST variability that is stronger, and emerges sooner, in the EP relative to the CP (*11*, *29*).

Despite the emerging view that ENSO SST variability will increase under anthropogenic forcing, underlying mechanisms and trajectories differ among models, highlighting that we lack unambiguous physical understanding of simulated changes (*30*). Improving the observational record will help identify models that best capture observed patterns and may be more likely to accurately assess future variability. High-resolution paleodata from the tropical Pacific fill a critical gap in defining long-term baselines and patterns of ENSO variability.

ENSO paleo-records from Galápagos corals

Here we use modern and subfossil Galápagos coral samples to quantify changes in interannual SST variance across the past millennium in the eastern equatorial Pacific (table S1). The Galápagos archipelago lies in the heart of the EP ENSO mode (Fig. 1), where the strongest basin-wide ENSO extremes with the greatest global impacts create maximum SST anomalies. Interannual variability in Galápagos SST reflects ENSO dynamics through changes in thermocline depth, upwelling, and advection. Coral skeletal Sr/Ca and $\delta^{18}O$ closely track past Galápagos SST (*31*–*34*). In the main archipelago, seawater $\delta^{18}O$ ($\delta^{18}O_{sw}$) variations are subtle and reflect circulation changes, not freshwater balance (*35*). Coral Sr/Ca and $\delta^{18}O$ are reproducible and correlate significantly with local and large-scale SST patterns, supporting their interpretation as EP-ENSO proxies (figs. S2 and S3).

We use coral Sr/Ca and $\delta^{18}O$ to characterize SST variations over the past millennium. Our results derive from analysis of 28 time series at 5 islands across the Galápagos archipelago (Fig. 1, tables S1 to S3, and figs. S4 and S5), using local SST-geochemistry calibrations (tables S4 and S5 and fig. S6). We empirically account for SST mean and variability gradients across the region (Fig. 1, fig. S7, and table S3) and calculate interannual SST variability based on filtered bimonthly SST anomalies reconstructed from coral Sr/Ca and $\delta^{18}O$ [supplementary materials (SM), materials and methods]. We quantify the change in variability from a modern benchmark period (Table 1 and table S6) and compare our results to central Pacific coral data (table S7) and other ENSO reconstructions using this "percent change" metric.

To assess whether our results exceed the range expected from internal variability or natural forcing, we compare coral-reconstructed changes with simulations of the preindustrial last millennium (850-1850 CE) driven by natural forcings (*36*–*38*), and their corresponding preindustrial control simulations. Our analysis incorporates twelve different climate models (table S8 and figs. S8 to S13), eleven of which are CMIP5/PMIP3 or CMIP6/PMIP4 members with one last-millennium simulation. The twelfth is the CESM Last Millennium Ensemble (LME), with 13 fully forced simulations of the last millennium (SM materials and methods).

Results: Increasing variability and asymmetry in eastern Pacific SST

Over the past millennium, EP-ENSO variability recorded in Galápagos corals parallels global temperature, with striking amplification in the last ~40 years (Figs. 1 and 2). Relatively low and consistent variance characterizes the 1000-1850 CE interval (hereafter "preindustrial"). In the following period (1850-1981; "20th century"), variability begins to rise in the late 19th century, emerging above the preindustrial range by the late 20th century. SST variability in the "modern" (since 1984) is consistently above that reconstructed during the preindustrial. Modern SST variability in the eastern equatorial Pacific is exceptional compared to the background state of this naturally dynamic system.

The coral reconstructions also track rising skewness (Fig. 1 and fig. S14) of EP-SST that reflects more frequent strong El Niño events. The skewness data are noisier than the variability results, but the shift from mostly neutral skewness in the preindustrial, to mostly positive skewness in the modern interval, indicates that stronger warm events underlie increased variance (Fig. 2). In the instrumental era, changes in coral and instrumental SST skewness track one another across the 20th century, although a recent decrease in coral skewness precedes a similar change in the instrumental record.

Each of the three intervals (Fig. 1) (pre-industrial, 20th-century, and modern) exhibits variability that is statistically distinct from the others, increasing through time (SM materials and methods and table S9) ($P \leq 0.0001$). Using the percent change in standard deviation, normalized to a recent 20-yr interval, we find that modern EP ENSO is 36.5 (±8)% stronger than in the pre-industrial, and 16.2 (±10)% stronger than in the 20th century (Table 1). Values in parentheses indicate the standard deviation among individual cores. Modern and 20th-century samples derive exclusively from the northernmost islands (Wolf and Darwin), and preindustrial samples derive mostly from the central archipelago (Fig. 1). Geographic normalization (SM materials and methods) corrects for variability differences that reflect distance from upwelling centers (fig. S7), but even without this correction, the modern epoch exhibits significantly higher variability ($P <$ 0.0001) than the earlier intervals (fig. S15 and table S9). At Isla Wolf, data from 4 colonies spanning preindustrial, 20th-century, and modern epochs confirm that the dramatic increase in SST variability is independent of site corrections.

Our analysis of last-millennium $\delta^{18}O$ data from Line Islands corals (table S7) extends and largely agrees with earlier work (*24*). Before 1850 CE, the range of variability among records is larger in the Line Islands than in the Galápagos, and preindustrial variability sometimes overlaps with modern ranges (Fig. 2). Nevertheless, modern Line Islands variability (which includes substantial seawater $\delta^{18}O$ influence) (*39*) is greater than preindustrial by 33.8 (±15)%, consistent with Galápagos results, and mean values of percent change are statistically distinct among epochs ($P < 0.0001$) (Table 1 and table S10).

Fossil coral records from the eastern Indian and western Pacific (Sumatra and Vanuatu) show increasing interannual variance over the past millennium that has been attributed to ENSO (*26*, *40*). The reconstructed changes in variability span the same range as Galápagos and Line Islands data, but do not show the clear distinction between preindustrial and modern seen at Galápagos (Fig. 2). Continuous ENSO reconstructions that merge a wider spatial network of coral, tree-ring and other paleodata (*20*, *41*, *42*) show increasing variance in the mid-19th century (fig. S16), preceding the Galápagos shift, and preindustrial variability that spans a wider range than in the EP. By contrast, individual foraminifera analysis (IFA) from the eastern Pacific shows modest variability, lowest early in the record and peaking in the late 1700's (*43*).

Analysis of preindustrial EP ENSO variability in last-millennium simulations and their associated preindustrial control simulations (table S8) reveals that the Galápagos coral-reconstructed change is significantly greater than simulated ENSO changes due to natural forcing or internal variability ($P < 0.05$) (Fig. 3). The variability change reconstructed from Galápagos corals (36.5%) exceeds the 95% confidence interval defined by EP-ENSO SST in 1) a multimodel ensemble of 11 fully forced simulations of the preindustrial last millennium; 2) a single-model ensemble of 13 fully forced simulations of the preindustrial last millennium; and 3) a multimodel ensemble of preindustrial (1850) control simulations corresponding to the forced experiments.

Spatial diversity in the evolution of ENSO variance

Over the past millennium, eastern and central Pacific coral reconstructions roughly agree on the mean amplitude of ENSO variability change. Neither indicates coherent shifts concurrent with the extratropical Little Ice Age (ca. 1500-1850 CE) or Medieval (ca. 800-1350 CE) (*44*) eras, although coral coverage is sparse before 1500 CE. However, the EP and CP coral reconstructions differ in other ways. The Galápagos coral analysis reveals a tight range of preindustrial variability across cores and sites, and a pronounced distinction between modern/20th century and preindustrial variability. By contrast, the Line Islands records show a greater range in reconstructed ENSO variability throughout the preindustrial, and a less distinct emergence of recent changes above preindustrial.

This difference likely reflects the mix of factors that determine coral $\delta^{18}O$ in the EP and CP. In the Line Islands, interannual SST anomalies are relatively small, and coral $\delta^{18}O$ records a substantial $\delta^{18}O_{sw}$ component that varies among events and islands (*39*, *45*). By contrast, in Galápagos, larger interannual SST changes dominate the coral $\delta^{18}O$ signal, as supported by long-term $\delta^{18}O_{sw}$ monitoring and agreement between paired $\delta^{18}O$ and Sr/Ca records. Galápagos $\delta^{18}O_{sw}$ reflects circulation-driven changes that do not correlate with local SST or ENSO indices (*35*). The wider range of variability in Line Islands coral records likely results from substantial influence of $\delta^{18}O_{sw}$ (*45*), estimated at 30% (Kiritimati) to >50% (Palmyra) of the coral $\delta^{18}O$ signal during 2015, caused by circulation and rainfall variability (*39*, *46*). The $\delta^{18}O_{sw}$ signal cannot be separated from SST in Line Islands coral records with available data. Conceivably, gaps in datasets could also create differences between Galapagos and Line Island results; the Galápagos data sample 48% of the years between 1100-2015 CE, and the Line Islands sample 59% of this interval.

To the extent that these records reflect variability in EP (Galápagos) and CP (Line Islands) ENSO SST, they describe a pattern consistent with model inferences of EP-ENSO and CP-ENSO responses to external forcing. CMIP5/6 models tend to project forced increases in ENSO SST variability that are more consistent and emerge more rapidly in the EP than in the CP (*27*, *29*). This pattern can result from several interrelated features, among them a reduced zonal SST gradient, increased stratification due to warming and intensified rainfall, and the nonlinear Bjerknes feedback associated with eastern Pacific warming and convection (*27*–*29*, *47*). The coral reconstructions do not distinguish among mechanisms; they provide an independent set of observational constraints that contextualize model simulations.

Comparison with continuous and sedimentary ENSO reconstructions

Continuous ENSO reconstructions based on multiple overlapping records (*20*, *41*, *42*) suggest that ENSO variability increased notably before 1900 (fig. S16), well before substantial global warming and the EP-ENSO variability increase at Galápagos. This may reflect biases that would create this particular timing. First, age model errors of even a year cause misalignment of extreme years among records. Combining such records will damp interannual variance as age model errors accumulate downcore (*48*, *49*). The start of instrumental SST records in the mid to late 1800s provides a reference for coral data that reduce such errors from that time forward. Second, almost all coral records from within 5-10° of the equator, where ENSO variance dominates, begin between 1850-1900 CE; reconstructed interannual variance increases as these records join the reconstructions (*49*). The age-model bias is minimized in tree-ring-only ENSO reconstructions (*41*), but the scarcity of old tropical records remains a source of inhomogeneity. A third bias comes from using remote records that may be nonlinearly or inconsistently related to equatorial Pacific SST (*50–52*). Prior to the late 1800s, the continuous reconstructions do not consistently agree on the timing of changes in variability.

Individual foraminifera analysis (*43*) provides a different picture of past ENSO variability (fig. S16). Percent-change values range over ±20% compared to modern, with highest variability during the 1700's. Compared to other records, IFA suggests relatively quiescent behavior and no modern strengthening. However, in the eastern Pacific, this method (using surface-dwelling species) is more likely to reflect seasonal than interannual changes (*53*). In the last millennium data, the topmost sample has fewer individuals than the rest of the core, making identification of change from modern even more challenging (SM materials and methods).

The continuous records (*20*, *41*, *42*) show scales of variability comparable to coral data and concur that variability was higher in the most recent period relative to pre-industrial. These powerful points of agreement collectively support the recent strengthening of ENSO. However, the continuous records suggest that this strengthening started in the 19th century, prior to substantial anthropogenic forcing. The 19th-century rise in variability may reflect the age model misalignment and sample coverage biases inherent to those reconstructions – biases that are absent in the Galapagos coral data. Although sparse in the 19th century, the Galápagos data indicate that the largest increase in EP-ENSO SST variability did not begin until the mid-late 20th century, as global warming accelerated (Fig. 2), and that variability was low with little century-scale structure before that time. Fossil coral reconstructions lack the continuity of multi-site paleoclimate syntheses and sediment cores, but they provide an alternate and compelling view of last-millennium ENSO variability that avoids biases described above.

Comparison with naturally forced and internal ENSO variability

To compare simulated and reconstructed EP-ENSO variability, we use the percent-change value at the 95th percentile of the cumulative density function across all models, using the EP SST index defined for each simulation (table S8 and SM materials and methods). The coral-reconstructed SST variability is highly unusual ($P < 0.05$) compared to naturally forced and internal variability. This is true whether we use the full millennium-long simulations, or just the subset of years covered by the corals, to define model variability (Fig. 3 and fig. S17). The reconstructed increase in EP-ENSO exceeds the variability in the unforced control simulations at a level approaching 99% significance (Fig. 3).

EP-ENSO variability differs among models, particularly in two of the CMIP-5 models (95% confidence interval of 58% and 54% for GISS-ER2-R and MPI-ESM-P, respectively). In these simulations, spikes in standard deviation coincide with volcanic forcing (fig. S9). This behavior is not seen in other forced simulations, nor in the preindustrial controls. In control simulations, EP-ENSO variability is more consistent, with little difference between CMIP5 and CMIP6 generations (table S8), suggesting that forced responses, not internal variability, drive intermodel differences in EP-ENSO variability. As in earlier work (*18*, *23*), forcing does not generally lead to greater ENSO variability: the only models that show substantial differences in EP-ENSO SST variability between forced and control simulations are the two in which volcanic eruptions produce outsize responses. Eight of the 11 CMIP5/6 models show similar levels of variance between forced and control simulations (95% CI differences <10%) (table S8).

The individual ensemble members of the LME yield similar percent-change values (table S8), comparable to the multi-model ensemble and control simulations. Our multi-model approach provides a robust background of naturally forced and internal ENSO variability against which reconstructed changes in EP-ENSO stand out distinctly. A formal attribution study is beyond the scope of this paper, but a recent synthesis of simulated changes in ENSO variability concluded that anthropogenic forcing is likely responsible for post-1960 increases in eastern Pacific variability (*27*). Regarding detectability, in a study of 68 CMIP5/6 models (*29*), 63% show EP-ENSO variability rising above background levels between 1940-2100, with a mean emergence date of ~2030. Our coral data, although discontinuous, are consistent with these results, particularly with the models showing early emergence. Additional coral data from the eastern equatorial Pacific to fill in temporal gaps would provide a more robust basis for comparison.

Conclusions

We document an unambiguous increase in EP-ENSO SST variability since the 19th century, particularly in recent decades, that reflects the observed intensification of El Niño warm extremes and exceeds simulated internal and naturally forced variability. This amplification is consistent with Earth system model projections that ENSO-related SST variance will likely increase and emerge first in the eastern Pacific (*27*, *29*). We find that SST variance in the EP is rising above background variability more rapidly than expected from most model simulations, whereas in the CP, increasing variance is statistically distinct, but has not yet unambiguously exceeded that of the past millennium. These data describe a pre-industrial range of EP-ENSO SST variability across a time span far longer than the instrumental record, highlighting the extraordinary nature of recent EP SST variability compared to the past millennium. We find no evidence for changes in EP-ENSO variability associated with the Little Ice Age and Medieval climate eras.

These results have important implications for climate hazards. ENSO extremes impose tremendous economic costs, ecological damages, and human suffering globally (*2*, *3*). The impact of more frequent and extreme El Niño events, superimposed on background ocean warming, has been particularly devastating to coral reef ecosystems and to marine ecosystems more broadly (*54*–*56*). As climate warms, the hydroclimatic impacts of ENSO are expected to amplify regardless of changes in SST variability (*57*). Our results highlight that the underlying SST variability is also strengthening; if this trend continues, it will further intensify the impact of ENSO within and beyond the tropical Pacific. By demonstrating a clear increase in eastern Pacific ENSO variability under unprecedented anthropogenic forcing, our results provide a point of comparison for identifying climate model simulations that successfully capture this change, which may improve our ability to anticipate and prepare for future risks.

REFERENCES AND NOTES

1. M. J. McPhaden, T. Lee, S. Fournier, M. A. Balmaseda, *El Niño Southern Oscillation in a Changing Climate*, M. McPhaden, A. Santoso, W. Cai, Eds. (American Geophysical Union, 2020), pp. 39–63.
2. P. Lehodey *et al*., *El Niño Southern Oscillation in a Changing Climate*, M. McPhaden, A. Santoso, W. Cai, Eds. (American Geophysical Union, 2020), pp. 429–451.
3. L. Goddard, A. Gershunov, *El Niño Southern Oscillation in a Changing Climate*, M. McPhaden, A. Santoso, W. Cai, Eds. (American Geophysical Union, 2020), pp. 361–375.
4. W. J. Cai, A. Santoso, M. Collins, B. Dewitte, C. Karamperidou, J.-S. Kug, M. Lengaigne, M. J. McPhaden, M. F. Stuecker, A. S. Taschetto, A. Timmermann, L. Wu, S.-W. Yeh, G. Wang, B. Ng, F. Jia, Y. Yang, J. Ying, X.-T. Zheng, T. Bayr, J. R. Brown, A. Capotondi, K. M. Cobb, B. Gan, T. Geng, Y.-G. Ham, F.-F. Jin, H.-S. Jo, X. Li, X. Lin, S. McGregor, J.-H. Park, K. Stein, K. Yang, L. Zhang, W. Zhong, Changing El Nino-Southern Oscillation in a warming climate. *Nat. Rev. Earth Environ.* **2**, 628–644 (2021). doi:10.1038/s43017-021-00199-z
5. M. Collins, S.-I. An, W. Cai, A. Ganachaud, E. Guilyardi, F.-F. Jin, M. Jochum, M. Lengaigne, S. Power, A. Timmermann, G. Vecchi, A. Wittenberg, The impact of global warming on the tropical Pacific ocean and El Niño. *Nat. Geosci.* **3**, 391–397 (2010). doi:10.1038/ngeo868
6. W. Cai, L. Wu, M. Lengaigne, T. Li, S. McGregor, J.-S. Kug, J.-Y. Yu, M. F. Stuecker, A. Santoso, X. Li, Y.-G. Ham, Y. Chikamoto, B. Ng, M. J. McPhaden, Y. Du, D. Dommenget, F. Jia, J. B. Kajtar, N. Keenlyside, X. Lin, J.-J. Luo, M. Martín-Rey, Y. Ruprich-Robert, G. Wang, S.-P. Xie, Y. Yang, S. M. Kang, J.-Y. Choi, B. Gan, G.-I. Kim, C.-E. Kim, S. Kim, J.-H. Kim, P. Chang, Pantropical climate interactions. *Science* **363**, eaav4236 (2019). doi:10.1126/science.aav4236 Medline
7. J. Y. Lee *et al*., *Climate Change 2021: The Physical Science Basis. Contribution of Working Group I to the Sixth Assessment Report of the Intergovernmental Panel on Climate Change*, V. Masson-Delmotte *et al*., Eds. (Cambridge University Press, 2021).
8. J. Emile-Geay, K. M. Cobb, J. E. Cole, M. Elliot, F. Zhu, *El Niño Southern Oscillation in a Changing Climate*, M. McPhaden, A. Santoso, W. Cai, Eds. (American Geophysical Union, 2020), pp. 87–118.
9. A. T. Wittenberg, Are historical records sufficient to constrain ENSO simulations? *Geophys. Res. Lett.* **36**, 2009GL038710 (2009). doi:10.1029/2009GL038710
10. H. Y. Kao, J. Y. Yu, Contrasting Eastern-Pacific and Central-Pacific Types of ENSO. *J. Clim.* **22**, 615–632 (2009). doi:10.1175/2008JCLI2309.1
11. W. Cai, G. Wang, B. Dewitte, L. Wu, A. Santoso, K. Takahashi, Y. Yang, A. Carréric, M. J. McPhaden, Increased variability of eastern Pacific El Niño under greenhouse warming. *Nature* **564**, 201–206 (2018). doi:10.1038/s41586-018-0776-9 Medline
12. C. Deser, A. S. Phillips, M. A. Alexander, Twentieth century tropical sea surface temperature trends revisited. *Geophys. Res. Lett.* **37**, 2010GL043321 (2010). doi:10.1029/2010GL043321
13. B. Wang, X. Luo, Y.-M. Yang, W. Sun, M. A. Cane, W. Cai, S.-W. Yeh, J. Liu, Historical change of El Niño properties sheds light on future changes of extreme El Niño. *Proc. Natl. Acad. Sci. U.S.A.* **116**, 22512–22517 (2019). doi:10.1073/pnas.1911130116 Medline
14. R. Gan, Q. Liu, G. Huang, K. Hu, X. Li, Greenhouse warming and internal variability increase extreme and central Pacific El Niño frequency since 1980. *Nat. Commun.* **14**, 394 (2023). doi:10.1038/s41467-023-36053-7 Medline
15. J. S. Kug, F. F. Jin, S. I. An, Two Types of El Nino Events: Cold Tongue El Nino and Warm Pool El Nino. *J. Clim.* **22**, 1499–1515 (2009). doi:10.1175/2008JCLI2624.1
16. A. Capotondi, A. T. Wittenberg, J.-S. Kug, K. Takahashi, M. J. McPhaden, *El Niño Southern Oscillation in a Changing Climate*, M. McPhaden, A. Santoso, W. Cai, Eds. (American Geophysical Union, 2020), pp. 65–86.
17. K. Takahashi, A. G. Martínez, The very strong coastal El Nino in 1925 in the far-eastern Pacific. *Clim. Dyn.* **52**, 7389–7415 (2019). doi:10.1007/s00382-017-3702-1
18. S. Stevenson, A. Capotondi, J. Fasullo, B. Otto-Bliesner, Forced changes to twentieth century ENSO diversity in a last Millennium context. *Clim. Dyn.* **52**, 7359–7374 (2017). doi:10.1007/s00382-017-3573-5
19. C. Karamperidou, P. N. DiNezio, Holocene hydroclimatic variability in the tropical Pacific explained by changing ENSO diversity. *Nat. Commun.* **13**, 7244 (2022). doi:10.1038/s41467-022-34880-8 Medline
20. M. B. Freund, B. J. Henley, D. J. Karoly, H. V. McGregor, N. J. Abram, D. Dommenget, Higher frequency of Central Pacific El Nino events in recent decades relative to past centuries. *Nat. Geosci.* **12**, 450–455 (2019). doi:10.1038/s41561-019-0353-3
21. J. E. Cole, R. G. Fairbanks, G. T. Shen, Recent variability in the southern oscillation: Isotopic results from a tarawa atoll coral. *Science* **260**, 1790–1793 (1993). doi:10.1126/science.260.5115.1790 Medline
22. F. E. Urban, J. E. Cole, J. T. Overpeck, Influence of mean climate change on climate variability from a 155-year tropical Pacific coral record. *Nature* **407**, 989–993 (2000). doi:10.1038/35039597 Medline
23. K. M. Cobb, N. Westphal, H. R. Sayani, J. T. Watson, E. Di Lorenzo, H. Cheng, R. L. Edwards, C. D. Charles, Highly variable El Niño-Southern Oscillation throughout the Holocene. *Science* **339**, 67–70 (2013). doi:10.1126/science.1228246 Medline
24. P. R. Grothe, K. M. Cobb, G. Liguori, E. Di Lorenzo, A. Capotondi, Y. Lu, H. Cheng, R. L. Edwards, J. R. Southon, G. M. Santos, D. M. Deocampo, J. Lynch-Stieglitz, T. Chen, H. R. Sayani, D. M. Thompson, J. L. Conroy, A. L. Moore, K. Townsend, M. Hagos, G. O'Connor, L. T. Toth, Enhanced El Nino-Southern Oscillation Variability in Recent Decades. *Geophys. Res. Lett.* **47**, e2019GL083906 (2019). doi:10.1029/2019GL083906
25. I. S. Nurhati, K. M. Cobb, E. Di Lorenzo, Decadal-Scale SST and Salinity Variations in the Central Tropical Pacific: Signatures of Natural and Anthropogenic Climate Change. *J. Clim.* **24**, 3294–3308 (2011). doi:10.1175/2011JCLI3852.1
26. A. E. Lawman, T. M. Quinn, J. W. Partin, K. Thirumalai, F. W. Taylor, C.-C. Wu, T.-L. Yu, M. K. Gorman, C.-C. Shen, A Century of Reduced ENSO Variability During the Medieval Climate Anomaly. *Paleoceanogr. Paleoclimatol.* **35**, e2019PA003742 (2020). doi:10.1029/2019PA003742
27. W. J. Cai, B. Ng, T. Geng, F. Jia, L. Wu, G. Wang, Y. Liu, B. Gan, K. Yang, A. Santoso, X. Lin, Z. Li, Y. Liu, Y. Yang, F.-F. Jin, M. Collins, M. J. McPhaden, Anthropogenic impacts on twentieth-century ENSO variability changes. *Nat. Rev. Earth Environ.* **4**, 407–418 (2023). doi:10.1038/s43017-023-00427-8
28. N. Maher, R. C. J. Wills, P. DiNezio, J. Klavans, S. Milinski, S. C. Sanchez, S. Stevenson, M. F. Stuecker, X. Wu, The future of the El Nino-Southern Oscillation: Using large ensembles to illuminate time-varying responses and inter-model differences. *Earth Syst. Dyn.* **14**, 413–431 (2023). doi:10.5194/esd-14-413-2023
29. T. Geng, W. Cai, L. Wu, A. Santoso, G. Wang, Z. Jing, B. Gan, Y. Yang, S. Li, S. Wang, Z. Chen, M. J. McPhaden, Emergence of changing Central-Pacific and Eastern-Pacific El Niño-Southern Oscillation in a warming climate. *Nat. Commun.* **13**, 6616 (2022). doi:10.1038/s41467-022-33930-5 Medline
30. U. K. Heede, A. V. Fedorov, Towards understanding the robust strengthening of ENSO and more frequent extreme El Nino events in CMIP6 global warming simulations. *Clim. Dyn.* **61**, 3047–3060 (2023).

31. J. E. Cole, A. W. Tudhope, *Coral Reefs of the Eastern Tropical Pacific: Persistence and Loss in a Dynamic Environment*, vol. 8, P. W. Glynn, D. P. Manzello, I. C. Enochs, Eds. (Springer, 2017), pp. 535–548.
32. G. Jimenez, J. E. Cole, D. M. Thompson, A. W. Tudhope, Northern Galapagos Corals Reveal Twentieth Century Warming in the Eastern Tropical Pacific. *Geophys. Res. Lett.* **45**, 1981–1988 (2018). doi:10.1002/2017GL075323
33. R. B. Dunbar, G. M. Wellington, M. W. Colgan, P. W. Glynn, Eastern Pacific sea surface temperature since 1600 A.D.: The d18O record of climate variability in Galapagos corals. *Paleoceanography* **9**, 291–315 (1994). doi:10.1029/93PA03501
34. A. H. Cheung, J. E. Cole, D. M. Thompson, L. Vetter, G. Jimenez, A. W. Tudhope, Fidelity of the Coral Sr/Ca Paleothermometer Following Heat Stress in the Northern Galapagos. *Paleoceanogr. Paleoclimatol.* **36**, e2021PA004323 (2021). doi:10.1029/2021PA004323
35. J. L. Conroy, N. K. Murray, G. S. Patterson, A. I. G. Schore, I. Ikuru, J. E. Cole, D. Chillagana, F. Echeverria, Equatorial Undercurrent Influence on Surface Seawater δ18O Values in the Galápagos. *Geophys. Res. Lett.* **50**, e2022GL102074 (2023). doi:10.1029/2022GL102074
36. J. H. Jungclaus, E. Bard, M. Baroni, P. Braconnot, J. Cao, L. P. Chini, T. Egorova, M. Evans, J. F. González-Rouco, H. Goosse, G. C. Hurtt, F. Joos, J. O. Kaplan, M. Khodri, K. Klein Goldewijk, N. Krivova, A. N. LeGrande, S. J. Lorenz, J. Luterbacher, W. Man, A. C. Maycock, M. Meinshausen, A. Moberg, R. Muscheler, C. Nehrbass-Ahles, B. I. Otto-Bliesner, S. J. Phipps, J. Pongratz, E. Rozanov, G. A. Schmidt, H. Schmidt, W. Schmutz, A. Schurer, A. I. Shapiro, M. Sigl, J. E. Smerdon, S. K. Solanki, C. Timmreck, M. Toohey, I. G. Usoskin, S. Wagner, C.-J. Wu, K. L. Yeo, D. Zanchettin, Q. Zhang, E. Zorita, The PMIP4 contribution to CMIP6-Part 3: The last millennium, scientific objective, and experimental design for the PMIP4 past1000 simulations. *Geosci. Model Dev.* **10**, 4005–4033 (2017). doi:10.5194/gmd-10-4005-2017
37. B. L. Otto-Bliesner, E. C. Brady, J. Fasullo, A. Jahn, L. Landrum, S. Stevenson, N. Rosenbloom, A. Mai, G. Strand, Climate variability and change since 850 CE An ensemble approach with the Community Earth System Model. *Bull. Am. Meteorol. Soc.* **97**, 735–754 (2016). doi:10.1175/BAMS-D-14-00233.1
38. G. Schmidt, J. H. Jungclaus, C. M. Ammann, E. Bard, P. Braconnot, T. J. Crowley, G. Delaygue, F. Joos, N. A. Krivova, R. Muscheler, B. L. Otto-Bliesner, J. Pongratz, D. T. Shindell, S. K. Solanki, F. Steinhilber, L. E. A. Vieira, Climate forcing reconstructions for use in PMIP simulations of the Last Millennium (v1.1). *Geosci. Model Dev.* **5**, 185–191 (2012). doi:10.5194/gmd-5-185-2012
39. S. Stevenson, K. M. Cobb, M. Merrifield, B. Powell, S. Sanchez, J. Nusbaumer, G. O'Connor, A. Atwood, Contrasting Central Equatorial Pacific Oxygen Isotopic Signatures of the 2014/2015 and 2015/2016 El Niño Events. *Geophys. Res. Lett.* **50**, e2023GL104454 (2023). doi:10.1029/2023GL104454
40. N. J. Abram, N. M. Wright, B. Ellis, B. C. Dixon, J. B. Wurtzel, M. H. England, C. C. Ummenhofer, B. Philibosian, S. Y. Cahyarini, T.-L. Yu, C.-C. Shen, H. Cheng, R. L. Edwards, D. Heslop, Coupling of Indo-Pacific climate variability over the last millennium. *Nature* **579**, 385–392 (2020). doi:10.1038/s41586-020-2084-4 Medline
41. J. B. Li, S.-P. Xie, E. R. Cook, M. S. Morales, D. A. Christie, N. C. Johnson, F. Chen, R. D'Arrigo, A. M. Fowler, X. Gou, K. Fang, El Nino modulations over the past seven centuries. *Nat. Clim. Chang.* **3**, 822–826 (2013). doi:10.1038/nclimate1936
42. J. Emile-Geay, K. M. Cobb, M. E. Mann, A. T. Wittenberg, Estimating Central Equatorial Pacific SST Variability over the Past Millennium. Part II: Reconstructions and Implications. *J. Clim.* **26**, 2329–2352 (2013). doi:10.1175/JCLI-D-11-00511.1
43. G. T. Rustic, A. Koutavas, T. M. Marchitto, B. K. Linsley, Dynamical excitation of the tropical Pacific Ocean and ENSO variability by Little Ice Age cooling. *Science* **350**, 1537–1541 (2015). doi:10.1126/science.aac9937 Medline
44. M. E. Mann, Z. Zhang, S. Rutherford, R. S. Bradley, M. K. Hughes, D. Shindell, C. Ammann, G. Faluvegi, F. Ni, Global signatures and dynamical origins of the Little Ice Age and Medieval Climate Anomaly. *Science* **326**, 1256–1260 (2009). doi:10.1126/science.1177303 Medline
45. D. M. Thompson, J. L. Conroy, B. L. Konecky, S. Stevenson, K. L. DeLong, N. McKay, E. Reed, L. Jonkers, M. Carré, Identifying hydro-sensitive coral δ18O records for improved high-resolution temperature and salinity reconstructions. *Geophys. Res. Lett.* **49**, e2021GL096153 (2022). doi:10.1029/2021GL096153
46. G. K. O'Connor, K. M. Cobb, H. R. Sayani, A. R. Atwood, P. R. Grothe, S. Stevenson, J. K. Baum, T. Chen, D. C. Claar, N. T. Hitt, J. Lynch-Stieglitz, R. A. Mortlock, G. A. Schmidt, R. Walter, Coral Oxygen Isotopic Records Capture the 2015/2016 El Nino Event in the Central Equatorial Pacific. *Geophys. Res. Lett.* **48**, e2021GL094036 (2021). doi:10.1029/2021GL094036
47. H. B. Fredriksen, J. Berner, A. C. Subramanian, A. Capotondi, How Does El Nino-Southern Oscillation Change Under Global Warming-A First Look at CMIP6. *Geophys. Res. Lett.* **47**, e2020GL090640 (2020). doi:10.1029/2020GL090640
48. M. Comboul, J. Emile-Geay, M. N. Evans, N. Mirnateghi, K. M. Cobb, D. M. Thompson, A probabilistic model of chronological errors in layer-counted climate proxies: Applications to annually banded coral archives. *Clim. Past* **10**, 825–841 (2014). doi:10.5194/cp-10-825-2014
49. G. Loope, D. M. Thompson, J. E. Cole, J. T. Overpeck, Is there a low-frequency bias in multiproxy reconstructions of tropical pacific SST variability? *Quat. Sci. Rev.* **246**, 106530 (2020). doi:10.1016/j.quascirev.2020.106530
50. J. E. Cole, E. R. Cook, The changing relationship between ENSO variability and moisture balance in the continental United States. *Geophys. Res. Lett.* **25**, 4529–4532 (1998). doi:10.1029/1998GL900145
51. S. C. Lewis, A. N. LeGrande, Stability of ENSO and its tropical Pacific teleconnections over the Last Millennium. *Clim. Past* **11**, 1347–1360 (2015). doi:10.5194/cp-11-1347-2015
52. A. J. E. Gallant, S. J. Phipps, D. Karoly, A. B. Mullan, A. M. Lorrey, Non-stationary Australasian teleconnections and implications for paleoclimate reconstructions. *J. Clim.* **26**, 8827–8849 (2013). doi:10.1175/JCLI-D-12-00338.1
53. K. Thirumalai, J. W. Partin, C. S. Jackson, T. M. Quinn, Statistical constraints on El Niño Southern Oscillation reconstructions using individual foraminifera: A sensitivity analysis. *Paleoceanography* **28**, 401–412 (2013). doi:10.1002/palo.20037
54. T. M. Clarke, C. C. C. Wabnitz, T. L. Frölicher, G. Reygondeau, D. Pauly, W. W. L. Cheung, Linking observed changes in pelagic catches to temperature and oxygen in the Eastern Tropical Pacific. *Fish Fish.* **23**, 1371–1382 (2022). doi:10.1111/faf.12694
55. N. J. Holbrook, A. Sen Gupta, E. C. J. Oliver, A. J. Hobday, J. A. Benthuysen, H. A. Scannell, D. A. Smale, T. Wernberg, Keeping pace with marine heatwaves. *Nat. Rev. Earth Environ.* **1**, 482–493 (2020). doi:10.1038/s43017-020-0068-4
56. T. P. Hughes, K. D. Anderson, S. R. Connolly, S. F. Heron, J. T. Kerry, J. M. Lough, A. H. Baird, J. K. Baum, M. L. Berumen, T. C. Bridge, D. C. Claar, C. M. Eakin, J. P. Gilmour, N. A. J. Graham, H. Harrison, J. A. Hobbs, A. S. Hoey, M. Hoogenboom, R. J. Lowe, M. T. McCulloch, J. M. Pandolfi, M. Pratchett, V. Schoepf, G. Torda, S. K. Wilson, Spatial and temporal patterns of mass bleaching of corals in the Anthropocene. *Science* **359**, 80–83 (2018). doi:10.1126/science.aan8048 Medline
57. S. Power, F. Delage, C. Chung, G. Kociuba, K. Keay, Robust twenty-first-century projections of El Niño and related precipitation variability. *Nature* **502**, 541–545 (2013). doi:10.1038/nature12580 Medline
58. R. W. Reynolds, T. M. Smith, C. Liu, D. B. Chelton, K. S. Casey, M. G. Schlax, Daily high-resolution-blended analyses for sea surface temperature. *J. Clim.* **20**, 5473–5496 (2007). doi:10.1175/2007JCLI1824.1
59. N. A. Rayner, D. E. Parker, E. B. Horton, C. K. Folland, L. V. Alexander, D. P. Rowell, E. C. Kent, A. Kaplan, Global analyses of sea surface temperature, sea ice, and night marine air temperature since the late nineteenth century. *J. Geophys. Res.* **108** (D14), 4407 (2003). doi:10.1029/2002JD002670
60. R. Neukom, L. A. Barboza, M. P. Erb, F. Shi, J. Emile-Geay, M. N. Evans, J. Franke, D. S. Kaufman, L. Lücke, K. Rehfeld, A. Schurer, F. Zhu, S. Brönnimann, G. J. Hakim, B. J. Henley, F. C. Ljungqvist, N. McKay, V. Valler, L. von Gunten; PAGES 2k Consortium, Consistent multi-decadal variability in global temperature reconstructions and simulations over the Common Era. *Nat. Geosci.* **12**, 643–649 (2019). doi:10.1038/s41561-019-0400-0 Medline
61. K. Cowtan, R. G. Way, Coverage bias in the HadCRUT4 temperature series and its impact on recent temperature trends. *Q. J. R. Meteorol. Soc.* **140**, 1935–1944 (2014). doi:10.1002/qj.2297
62. E. R. M. Druffel, S. Griffin, D. Vetter, R. B. Dunbar, D. M. Mucciarone, Identification of frequent La Niña events during the early 1800s in the east equatorial Pacific. *Geophys. Res. Lett.* **42**, 1512–1519 (2015). doi:10.1002/2014GL062997

63. E. V. Reed, D. M. Thompson, J. E. Cole, J. M. Lough, N. E. Cantin, A. H. Cheung, A. Tudhope, L. Vetter, G. Jimenez, R. L. Edwards, Impacts of Coral Growth on Geochemistry: Lessons From the Galapagos Islands. *Paleoceanogr. Paleoclimatol.* **36**, e2020PA004051 (2021). doi:10.1029/2020PA004051
64. P. W. Glynn, State of Coral Reefs in the Galapagos Islands: Natural vs Anthropogenic Impacts. *Mar. Pollut. Bull.* **29**, 131–140 (1994). doi:10.1016/0025-326X(94)90437-5
65. P. W. Glynn, B. Riegl, A. M. S. Correa, I. B. Baums, Rapid recovery of a coral reef at Darwin Island, Galapagos Islands. *Galapagos Res.* **66**, 6–13 (2009).
66. K. Thirumalai, A. Singh, R. Ramesh, A MATLAB™ code to perform weighted linear regression with (correlated or uncorrelated) errors in bivariate data. *J. Geol. Soc. India* **77**, 377–380 (2011). doi:10.1007/s12594-011-0044-1
67. G. M. Wellington, R. B. Dunbar, G. Merlen, Calibration of stable oxygen isotope signatures in Galápagos corals. *Paleoceanography* **11**, 467–480 (1996). doi:10.1029/96PA01023
68. D. York, N. M. Evensen, M. L. Martínez, J. De Basabe Delgado, Unified equations for the slope, intercept, and standard errors of the best straight line. *Am. J. Phys.* **72**, 367–375 (2004). doi:10.1119/1.1632486
69. W. Ebisuzaki, A method to estimate the statistical significance of a correlation when the data are serially correlated. *J. Clim.* **10**, 2147–2153 (1997). doi:10.1175/1520-0442(1997)010<2147:AMTETS>2.0.CO;2
70. B. Huang, P. W. Thorne, V. F. Banzon, T. Boyer, G. Chepurin, J. H. Lawrimore, M. J. Menne, T. M. Smith, R. S. Vose, H.-M. Zhang, Extended Reconstructed Sea Surface Temperature, Version 5 (ERSSTv5): Upgrades, Validations, and Intercomparisons. *J. Clim.* **30**, 8179–8205 (2017). doi:10.1175/JCLI-D-16-0836.1
71. M. Toohey, B. Stevens, H. Schmidt, C. Timmreck, Easy Volcanic Aerosol (EVA v1. 0): An idealized forcing generator for climate simulations. *Geosci. Model Dev.* **9**, 4049–4070 (2016). doi:10.5194/gmd-9-4049-2016
72. A. H. Jaffey, K. F. Flynn, L. E. Glendenin, W. C. Bentley, A. M. Essling, Precision measurement of half-lives and specific activities of U-235 and U-238. *Phys. Rev. C Nucl. Phys.* **4**, 1889–1906 (1971). doi:10.1103/PhysRevC.4.1889
73. H. Cheng, R. Lawrence Edwards, C.-C. Shen, V. J. Polyak, Y. Asmerom, J. Woodhead, J. Hellstrom, Y. Wang, X. Kong, C. Spötl, X. Wang, E. Calvin Alexander Jr., Improvements in Th-230 dating, Th-230 and U-234 half-life values, and U-Th isotopic measurements by multi-collector inductively coupled plasma mass spectrometry. *Earth Planet. Sci. Lett.* **371-372**, 82–91 (2013). doi:10.1016/j.epsl.2013.04.006
74. S. C. Sanchez, N. Westphal, G. H. Haug, H. Cheng, R. L. Edwards, T. Schneider, K. M. Cobb, C. D. Charles, A Continuous Record of Central Tropical Pacific Climate Since the Midnineteenth Century Reconstructed From Fanning and Palmyra Island Corals: A Case Study in Coral Data Reanalysis. *Paleoceanogr. Paleoclimatol.* **35**, e2020PA003848 (2020). doi:10.1029/2020PA003848
75. K. M. Cobb, C. D. Charles, H. Cheng, R. L. Edwards, El Niño/Southern Oscillation and tropical Pacific climate during the last millennium. *Nature* **424**, 271–276 (2003). doi:10.1038/nature01779 Medline
76. I. S. Nurhati, K. M. Cobb, C. D. Charles, R. B. Dunbar, Late 20th century warming and freshening in the central tropical Pacific. *Geophys. Res. Lett.* **36**, 2009GL040270 (2009). doi:10.1029/2009GL040270
77. S. G. Dee, K. M. Cobb, J. Emile-Geay, T. R. Ault, R. L. Edwards, H. Cheng, C. D. Charles, No consistent ENSO response to volcanic forcing over the last millennium. *Science* **367**, 1477–1481 (2020). doi:10.1126/science.aax2000 Medline
78. K. M. Cobb, C. D. Charles, D. E. Hunter, A central tropical Pacific coral demonstrates Pacific, Indian, and Atlantic decadal climate connections. *Geophys. Res. Lett.* **28**, 2209–2212 (2001). doi:10.1029/2001GL012919
79. L. K. Zaunbrecher, K. M. Cobb, J. W. Beck, C. D. Charles, E. R. M. Druffel, R. G. Fairbanks, S. Griffin, H. R. Sayani, Coral records of central tropical Pacific radiocarbon variability during the last millennium. *Paleoceanography* **25**, PA4212 (2010). doi:10.1029/2009PA001788
80. M. Evans, R. G. Fairbanks, J. L. Rubenstone, A proxy index of ENSO teleconnections. *Nature* **394**, 732–733 (1998). doi:10.1038/29424
81. T. W. Wu *et al*., An Overview of BCC Climate System Model Development and Application for Climate Change Studies. *J. Meteorol. Res.* **28**, 34–56 (2014).
82. L. Landrum, B. L. Otto-Bliesner, E. R. Wahl, A. Conley, P. J. Lawrence, N. Rosenbloom, H. Teng, Last Millennium Climate and Its Variability in CCSM4. *J. Clim.* **26**, 1085–1111 (2013). doi:10.1175/JCLI-D-11-00326.1
83. G. A. Schmidt, R. Ruedy, J. E. Hansen, I. Aleinov, N. Bell, M. Bauer, S. Bauer, B. Cairns, V. Canuto, Y. Cheng, A. Del Genio, G. Faluvegi, A. D. Friend, T. M. Hall, Y. Hu, M. Kelley, N. Y. Kiang, D. Koch, A. A. Lacis, J. Lerner, K. K. Lo, R. L. Miller, L. Nazarenko, V. Oinas, J. Perlwitz, J. Perlwitz, D. Rind, A. Romanou, G. L. Russell, M. Sato, D. T. Shindell, P. H. Stone, S. Sun, N. Tausnev, D. Thresher, M.-S. Yao, Present-day atmospheric simulations using GISS ModelE: Comparison to in situ, satellite, and reanalysis data. *J. Clim.* **19**, 153–192 (2006). doi:10.1175/JCLI3612.1
84. F. Hourdin, M.-A. Foujols, F. Codron, V. Guemas, J.-L. Dufresne, S. Bony, S. Denvil, L. Guez, F. Lott, J. Ghattas, P. Braconnot, O. Marti, Y. Meurdesoif, L. Bopp, Impact of the LMDZ atmospheric grid configuration on the climate and sensitivity of the IPSL-CM5A coupled model. *Clim. Dyn.* **40**, 2167–2192 (2013). doi:10.1007/s00382-012-1411-3
85. T. Sueyoshi, R. Ohgaito, A. Yamamoto, M. O. Chikamoto, T. Hajima, H. Okajima, M. Yoshimori, M. Abe, R. O'ishi, F. Saito, S. Watanabe, M. Kawamiya, A. Abe-Ouchi, Set-up of the PMIP3 paleoclimate experiments conducted using an Earth system model, MIROC-ESM. *Geosci. Model Dev.* **6**, 819–836 (2013). doi:10.5194/gmd-6-819-2013
86. J. H. Jungclaus, S. J. Lorenz, C. Timmreck, C. H. Reick, V. Brovkin, K. Six, J. Segschneider, M. A. Giorgetta, T. J. Crowley, J. Pongratz, N. A. Krivova, L. E. Vieira, S. K. Solanki, D. Klocke, M. Botzet, M. Esch, V. Gayler, H. Haak, T. J. Raddatz, E. Roeckner, R. Schnur, H. Widmann, M. Claussen, B. Stevens, J. Marotzke, Climate and carbon-cycle variability over the last millennium. *Clim. Past* **6**, 723–737 (2010). doi:10.5194/cp-6-723-2010
87. S. Yukimoto, Y. Adachi, M. Hosaka, T. Sakami, H. Yoshimura, M. Hirabara, T. Y. Tanaka, E. Shindo, H. Tsujino, M. Deushi, R. Mizuta, S. Yabu, A. Obata, H. Nakano, T. Koshiro, T. Ose, A. Kitoh, A New Global Climate Model of the Meteorological Research Institute: MRI-CGCM3-Model Description and Basic Performance. *J. Meteorol. Soc. Jpn.* **90A**, 23–64 (2012). doi:10.2151/jmsj.2012-A02
88. L. R. Marshall, A. Schmidt, A. P. Schurer, N. L. Abraham, L. J. Lücke, R. Wilson, K. J. Anchukaitis, G. C. Hegerl, B. Johnson, B. L. Otto-Bliesner, E. C. Brady, M. Khodri, K. Yoshida, Last-millennium volcanic forcing and climate response using SO2 emissions. *Clim. Past* **21**, 161–184 (2025). doi:10.5194/cp-21-161-2025
89. T. Hajima, M. Watanabe, A. Yamamoto, H. Tatebe, M. A. Noguchi, M. Abe, R. Ohgaito, A. Ito, D. Yamazaki, H. Okajima, A. Ito, K. Takata, K. Ogochi, S. Watanabe, M. Kawamiya, Development of the MIROC-ES2L Earth system model and the evaluation of biogeochemical processes and feedbacks. *Geosci. Model Dev.* **13**, 2197–2244 (2020). doi:10.5194/gmd-13-2197-2020
90. O. Gutjahr, D. Putrasahan, K. Lohmann, J. H. Jungclaus, J.-S. von Storch, N. Brüggemann, H. Haak, A. Stössel, Max Planck Institute Earth System Model (MPI-ESM1.2) for the High-Resolution Model Intercomparison Project (HighResMIP). *Geosci. Model Dev.* **12**, 3241–3281 (2019). doi:10.5194/gmd-12-3241-2019
91. S. Yukimoto, H. Kawai, T. Koshiro, N. Oshima, K. Yoshida, S. Urakawa, H. Tsujino, M. Deushi, T. Tanaka, M. Hosaka, S. Yabu, H. Yoshimura, E. Shindo, R. Mizuta, A. Obata, Y. Adachi, M. Ishii, The Meteorological Research Institute Earth System Model Version 2.0, MRI-ESM2.0: Description and Basic Evaluation of the Physical Component. *J. Meteorol. Soc. Jpn.* **97**, 931–965 (2019). doi:10.2151/jmsj.2019-051

ACKNOWLEDGMENTS

We are deeply grateful to the Galápagos National Park, particularly G. Quezada, D. Rueda, and J. Suarez, for permission and support for our work in this special place, and to the Charles Darwin Research Station, notably M. Romoleroux, S. Cisneros, and S. Rea, for facilitating this work. We could not have done this project without robust field support from L. Cruz, R. Pepolas, and E. Romero. P. Glynn and S. Banks advised us on modern Galápagos reefs. We appreciate field and lab assistance from S. Hlohowskyj, M. Wilson, D. Ruiz, S. Villareal, A. Lema, S. Lemieux, M. Nicholson, S. Acosta, D. Dettman, C. Garton, C. Kotila, J. McCraw, and M. Snyder. K. Thirumalai and J. C. Overpeck provided invaluable statistical guidance. This publication is contribution number 2780 of the Charles Darwin Foundation for the Galápagos Islands, and the work was conducted under Galápagos National Park permits PC-17-06, PC-24-10, PC-01-15, and PC-45-16. **Funding:** US National Science Foundation grants OCE 0957881, OCE 1401326, OCE 1829613 (J.E.C.); US National Science Foundation grant AGS 1561121 (D.M.T.); US National Science Foundation grant AGS 2002460 (D.M.T. and M.L.); US National Science Foundation grant AGS 1847791 (J.L.C.); US National Science Foundation grants OCE 2142953, OCE 2202794, AGS 1805143 (S.S.); and UK Natural Environmental Research Council grant NERC NE/H009957/1 (A.W.T.). **Author contributions:** Conceptualization: J.E.C., A.W.T., D.M.T. Funding acquisition: J.E.C., A.W.T., D.M.T. Methodology: J.E.C., D.M.T., A.W.T., K.A.D., S.S., M.L., A.E.L. Formal Analysis: J.E.C., C.J.T., D.M.T., M.L., A.E.L., J.M.O. Investigation: K.A.D., J.M.O., G.J., R.L.E., J.E.C. Visualization: J.E.C., K.A.D., D.M.T., C.J.T., M.L. Project administration: J.E.C. Supervision: J.E.C. Writing – original draft: J.E.C., D.M.T., S.S., M.L., K.A.D. Writing – review & editing: all authors. **Competing interests:** The authors declare that they have no competing interests. **Data, code, and materials availability:** Data are available at the NOAA-NCEI World Data Service for Paleoclimatology: https://www.ncei.noaa.gov/access/paleo-search/study/43983. No new materials were generated for this study.

SUPPLEMENTARY MATERIALS

science.org/doi/10.1126/science.ady2660
Materials and Methods
Figs. S1 to S17
Tables S1 to S10
References (*62*–*91*)

Submitted 16 April 2025; accepted 12 August 2026
Published online 27 August 2026
10.1126/science.ady2660

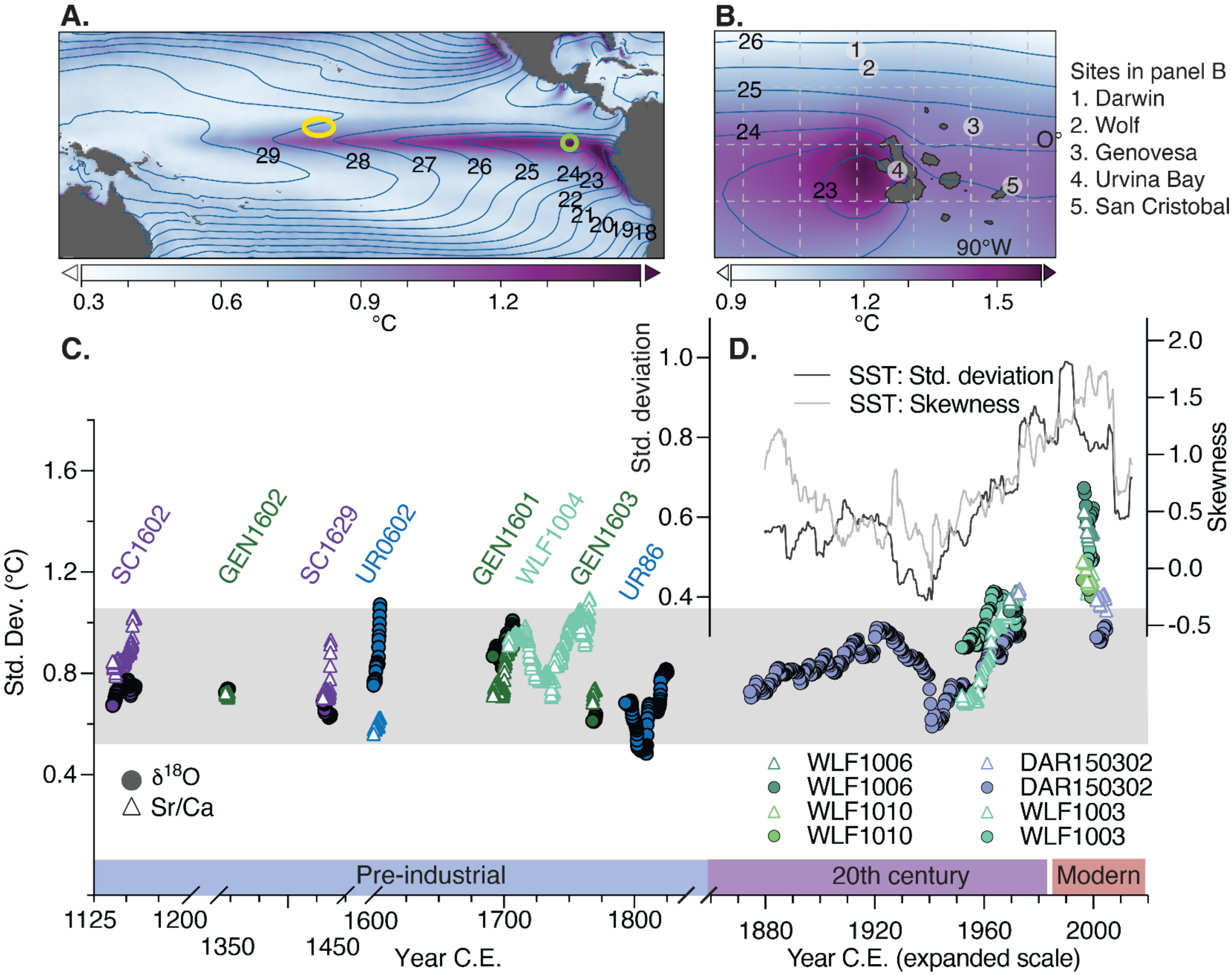

Fig. 1. Eastern Pacific SST variability, modern and last millennium. (A) Standard deviation of observed monthly SST anomalies (1982-2024; colors), superimposed on mean SST (labeled contours in °C). The Galápagos and Line Island archipelagos are indicated by green and yellow symbols, respectively. (B) As in A, but for Galápagos archipelago (note different scaling). Coral sites are numbered. Data accessed from OISSTv2.1 product (*58*) using Climate Explorer (https://climexp.knmi.nl). (C) Colored symbols represent the 20-yr running standard deviation of interannual SST anomalies reconstructed from Galápagos corals, corrected for inter-island offsets. Circles represent coral $\delta^{18}O$-derived SST variability and triangles indicate SST variability derived from coral Sr/Ca. Time series lose 10 years off their start and end dates due to the 20-yr running calculation, and the gap centered in the1980's results from the death horizon in all modern Galápagos corals. Pre-industrial corals are labeled with sample IDs; post-1860 samples are identified in legend. Shaded grey range indicates $\pm 2\sigma$ range (95% distribution) for pre-industrial variability. Note the discontinuous X-axis. (D) Inset plot shows the 20-year running standard deviation for instrumental Galápagos SST in dark grey and the running 20-yr skewness of interannual anomalies in light grey (HadISST: 2°S-2°N, 88-92°W) (*59*). Shaded bars at bottom indicate preindustrial, 20th-century, and modern epochs. SST and coral data are processed as in the SM materials and methods.

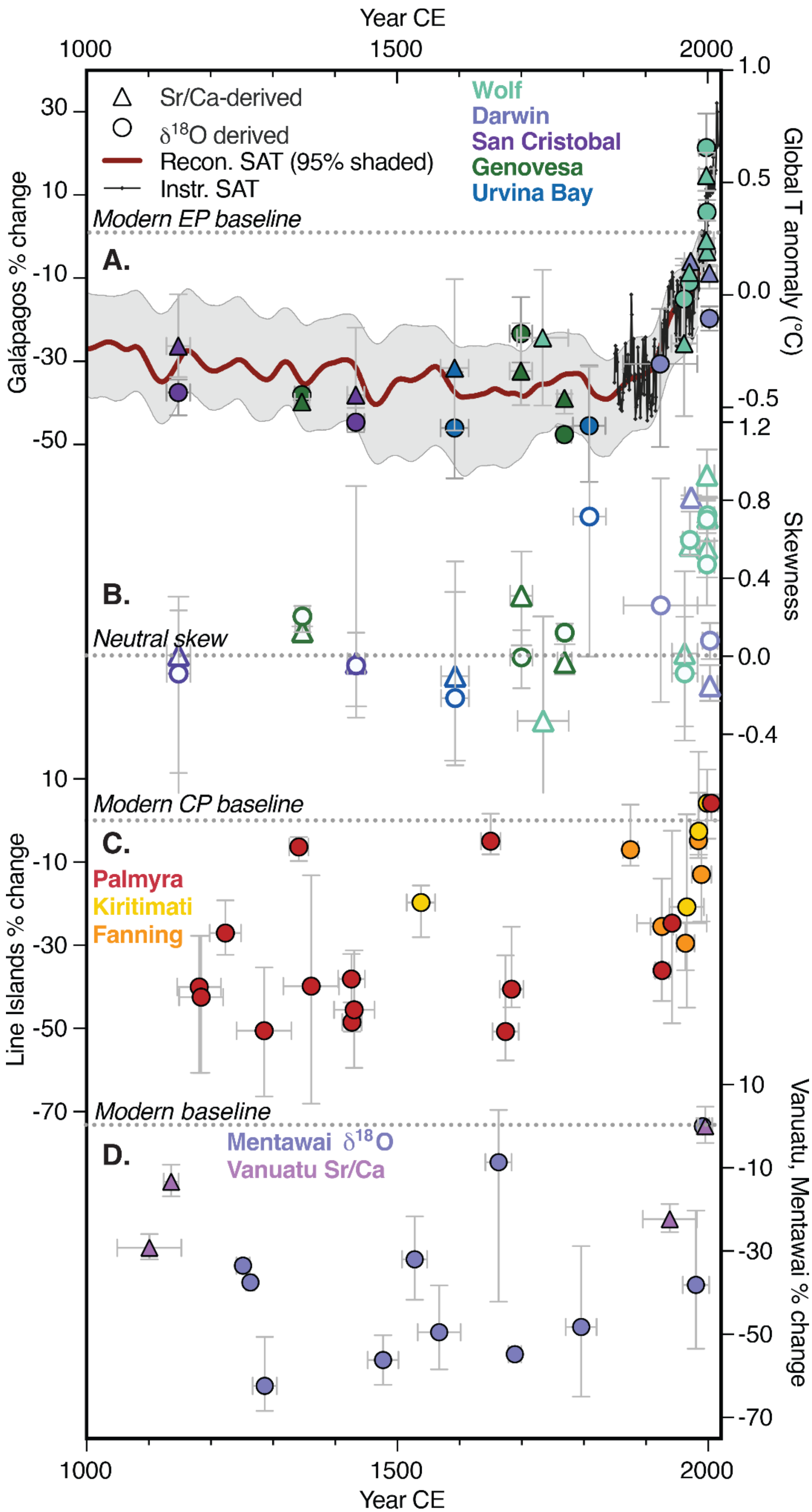

Fig. 2. Comparison of coral-reconstructed interannual variability in the Indo-Pacific and global surface air temperature (SAT). (**A**) Change in interannual SST variability from Galápagos corals, expressed as percentage change from modern. Each symbol represents a single record: colors represent different islands, and shapes indicate proxy type (circles: $\delta^{18}O$; triangles: Sr/Ca). Vertical and horizontal bars indicate ranges of percent change and ages, respectively. SAT change is indicated by black line (instrumental) and bold red line (reconstructed, with 95% confidence indicated by light grey shading) (*60*, *61*). (**B**) Skewness of Galápagos coral SST anomalies, shown with open symbols using the same color scheme as in A, and calculated on the same filtered SST anomaly data used for the running standard deviation metric. Vertical bars indicate minimum and maximum 20-yr running values, and horizontal bars reflect the total length of each coral record. (**C**) Change in interannual variability of coral $\delta^{18}O$ data from the northern Line Islands, expressed as percent change from modern as for A. Colors represent different islands as in legend. (**D**) Change in interannual variability of coral $\delta^{18}O$ data from Mentawai and Vanuatu, expressed as percent change from modern as for A. Colors represent different islands as in legend. Data sources in tables S1 and S7.

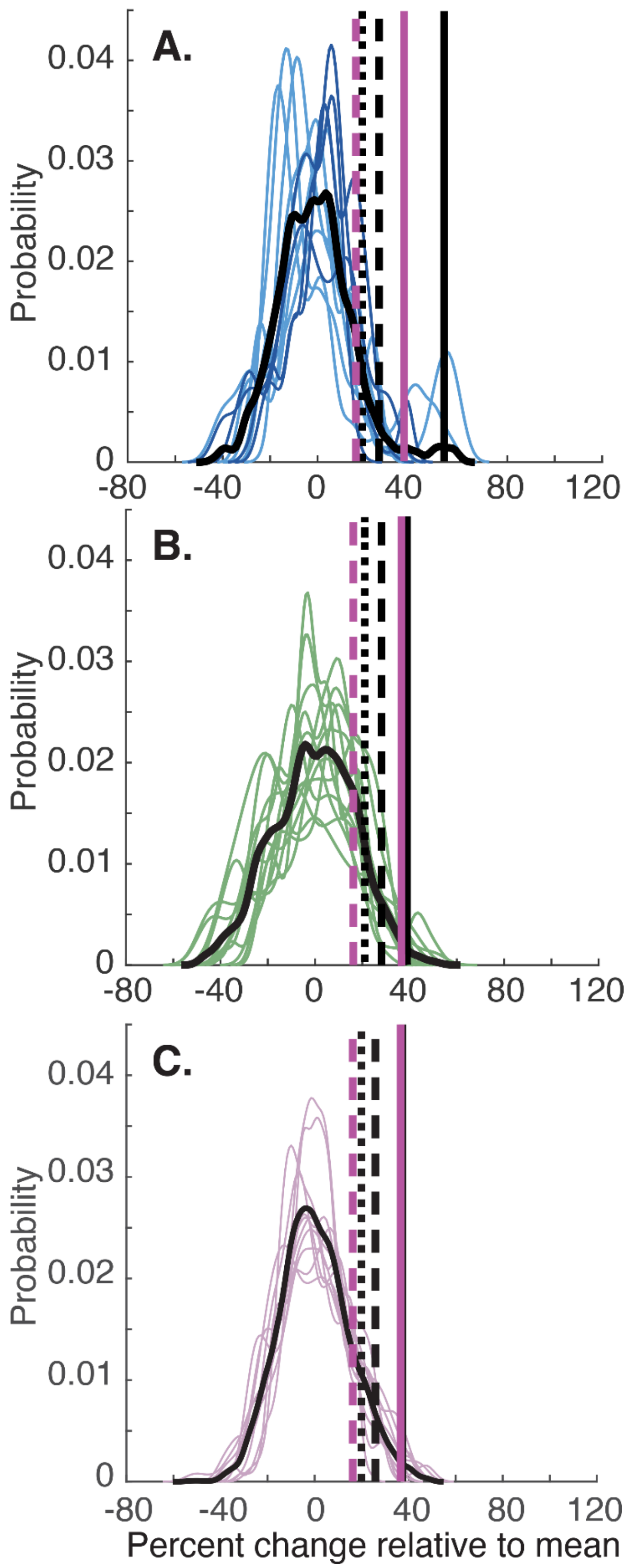

Fig. 3. Distribution of percent-change values for climate model simulations, compared to Galápagos coral. Each plot shows the distribution of percent-change values calculated for all 20-yr standard deviations in a simulation compared to the mean 20-year standard deviation. Vertical lines show the Galápagos coral changes in magenta (modern relative to PI solid, modern relative to 20th century dashed) and the model 90, 95, and 99% significance levels values in black dotted, dashed, and solid lines. (**A**) CMIP5 (light blue) and CMIP6 (dark blue) models; black is the mean of all. These are calculated for coral years only. (**B**) LME ensemble (individual members in green, mean in black). These are calculated for coral years only. (**C**) Pre-industrial control simulations for each of the CMIP5/6 models (individual models in pink; mean in black; 99% and coral modern-PI lines overlap). Values for control simulations are calculated over the full 500-year simulations. The distribution of percent change values over the full lengths of CMIP5/6 and LME simulations are provided in fig. S17.

Table 1. Percent change in ENSO variability compared to modern. Percent change is calculated for each coral record as the difference from the modern benchmark interval, using 20-yr standard deviation (SD20) values. Percent change = ((modern benchmark SD20 – older SD20)/modern benchmark SD20). Benchmark intervals are given in table S6, and statistical tests are described in the SM materials and methods with results in table S9. We compare the values in this table for Galápagos with model results in Fig. 3 and fig. S17.

	Preindustrial last millennium	Post-industrial ~20th century
Years	1000 to 1850 CE	1851 to 1982 CE
Galápagos	36.5% (±8); $P < 0.0001$	16.2% (±10); $P < 0.0001$
Line Islands	33.8% (±15); $P < 0.0001$	18.5% (±15); $P < 0.05$

Recent strengthening of eastern Pacific ENSO in the last millennium paleorecord

J. E. Cole, D. M. Thompson, K. A. Dyez, C. J. Tripp, A. W. Tudhope, M. Lofverstrom, S. Stevenson, J. M. Okun, A. E. Lawman, J. L. Conroy, J. T. Overpeck, G. Jimenez, and R. L. Edwards

Science **Ahead of Print** DOI: 10.1126/science.ady2660

Science (ISSN 1095-9203) is published by the American Association for the Advancement of Science. 1200 New York Avenue NW, Washington, DC 20005. The title *Science* is a registered trademark of AAAS.